CAPACITY OF SHORT PILES AND CAISSONS IN SOFT CLAY FROM GEOTECHNICAL CENTRIFUGE TESTS

Madhuri Murali[1], A.M., ASCE

Francisco J. Grajales S.[2] A.M., ASCE

Ryan D. Beemer[3] A.M., ASCE

Charles P. Aubeny[4], F., ASCE

Giovanna Biscontin[5], M., ASCE

ABSTRACT

Geotechnical centrifuge tests were conducted to examine the behavior of low aspect ratio piles and caissons in clayey soils subjected to high moment loading. Model piles with aspect ratio of two were tested in the 150g-ton centrifuge at Rensselaer Polytechnic Institute. Results include moment-inclination and force-displacement response for different loading conditions. Numerical studies were also performed consisting of three dimensional finite element simulations in order to predict capacities. The comparisons are performed in terms of the total resistance that is exerted by the soil on the caisson. This paper focuses on presenting the ultimate bearing capacity factors including both experimental and numerical results. In addition, results are compared to a series of studies available in the literature, which include upper bound solutions and experimental results.

Keywords: Geotechnical, Foundations, Caisson, Piles, Offshore, Centrifuge

[1]Project Engineer, Fugro Netherlands Marine, Prismastraat 4, 2631 RT, Nootdorp, Netherlands, Email: M.Murali@fugro.com.

[2]Assistant Professor, School of Civil Engineering, Universidad Tecnologica de Panama, Main Campus Victor L. Sasso, Panama City, Rep. of Panama E-mail: francisco.grajales@utp.ac.pa

[3]Postdoctoral Research Assoc., COFS University of Western Australia, 35 Stirling Highway, Crawley, WA 6009, Australia. E-mail: ryan.beemer@uwa.edu.au

[4]Professor, Zachry Dept. of Civil Engr., Dwight Look College of Engr., Texas A&M University, 3136 TAMU, College Station, TX 77843, USA. E-mail: caubeny@civil.tamu.edu.

[5]Lecturer, Department of Engineering, University of Cambridge, Schofield Centre, High Cross, Madingley Road, Cambridge CB3 0EL, UK. E-mail: gb479@cam.ac.uk.

INTRODUCTION

Pile and caisson foundations are commonly used in offshore applications. One advantage of the caisson foundation is its flexibility to be utilized as a stand-alone structure (eg. anchor) or to be utilized in a cluster (eg. tripods, jacket foundations) and provide rotational capacity and stiffness. The aspect ratio (length to diameter, L_f/D) of these caisson foundations (suction-installed piles) is typically less than 6 (Tjelta 2001). In this range of aspect ratios flexural response (bending) is negligible, so for some purposes the pile can be analyzed as a rotating-translating rigid body, which lends itself to the methods of plasticity theory for computation of load capacity. In normally consolidated clay profiles the optimal aspect ratio is typically on the order of L_f/D = 5. For these relatively high aspect ratios, predictions based on plasticity theory are in good agreement with both rigorous finite element solutions (Andersen et al. 2005) and centrifuge tests (Clukey et al. 2004). However, for short caissons, say $L_f/D < 3$, differences between upper bound plastic limit analyses and finite element solutions are greater (Andersen et al. 2005) and the database of physical measurements is relatively sparse. While general loading on shallowly embedded foundations with $L_f/D < 1$ has been the focus of considerable attention (Yun and Bransby 2007; Gourvenec 2008) and several noteworthy numerical studies present numerical predictions for the range L_f/D = 1 to 5 (Supachawarote et al. 2004; Palix et al. 2011), experimental validation is relatively limited in the intermediate range of aspect ratios L_f/D = 1-3.

One of the aims of this study is to provide experimental evidence through geotechnical centrifuge tests to validate numerical models and develop improved plastic solutions for short piles (or caissons) under combined loads. The centrifuge is an extremely useful tool to model self-weight stresses and gravity dependent processes as they are accurately reproduced allowing observations from small scale models to be related to the full scale prototype through well established scaling laws. The principles of centrifuge modeling have been discussed and thoroughly verified through numerous trials (Pokrovsky and Fyodorov 1936; Taylor, R. N. (ed.) 1995; Garnier and Gaudin 2007). Centrifuge testing has been extensively used to model offshore geotechnical problems in particular (Hamilton et al. 1991; Murff 1996; Clukey et al. 2004; Jeanjean 2009; Zhang et al. 2011;

Cassidy and Byrne 2001; Lau 2015).

This paper presents the findings of a series of centrifuge tests on suction caissons with aspect ratio L_f/D = 2 in normally to lightly over-consolidated kaolin. The tests included both pure horizontal translational loading and eccentric horizontal loads, applied above the mudline. The measurements of pure translational capacity as well as the trends in load capacity reduction due to load eccentricity have an application towards suction anchors in deep water mooring systems. The eccentric load conditions can also prove useful to renewable energy facilities utilizing the caisson foundation, such as offshore wind or tidal current turbines. Ultimate load capacity measurements are presented for monotonic loading in intact soil conditions and for monotonic loading following cyclic loading at small displacement levels. The test results are evaluated and interpreted through comparisons to finite element simulations (Grajales 2017) and plastic limit analyses (Murff and Hamilton 1993; Aubeny et al. 2001a; Aubeny et al. 2003).

BACKGROUND

Ultimate Horizontal Capacity

Murff and Hamilton (1993) presented a three dimensional upper bound plastic limit analysis method for the computation of the ultimate undrained capacity of horizontally loaded long piles. The failure mechanism comprises three regions: (1) a conical failure wedge that accounts for free surface effects, (2) a flow around zone (i.e. region where the caisson is translating, without the influence of surface effects) and (3) a spherical failure surface at the bottom of the caisson. The flow around region is described by the plane strain solution for a translating cylinder developed by Randolph and Houlsby (1984). The original analysis was performed by optimization of several variable parameters. Finally, a simplified expression for equivalent horizontal bearing factors (N_p) was proposed as shown in Eq.1:

$$N_p = \frac{\Delta F}{s_u D \Delta L_f} \tag{1}$$

where s_u is the undrained shear strength at the depth in question, D is the caisson diameter,

ΔL_f is an increment in length (depth) of the caisson, and ΔF is the increase in horizontal capacity (or soil resistance) corresponding to the successive increase in length (ΔL_f) for pure translation of the caisson. Murff and Hamilton (1993) also showed that the predicted horizontal soil-resistance profiles for rotating and translating caissons are similar (i.e. the resistance is independent of the location of the center of rotation). This is consistent with semi-empirical models or methods based on equivalent p-y curves (Matlock 1970; Reese et al. 1975). Murff and Hamilton (1993) also compared their bearing factors to centrifuge data by Hamilton et al. (1991) and found good agreement.

Based on Murff and Hamilton (1993) results, Aubeny et al. (2001a) developed a simplified plastic limit analysis for estimating the horizontal capacity of suction caissons and open ended piles which avoids solving the complex integrations required to model the original failure mechanism. This simplified method is applicable to both uniform or a linearly varying undrained shear strength profile. This method was extended to account for inclined loads (Aubeny et al. 2003), which are common when caissons are used as anchoring systems. The validity and limitations of the simplified formulation were also demonstrated through comparisons to rigorous finite element solutions.

Combined Loading

The behavior of piles and caissons subject to combined loading has been widely studied by a number of authors (Tan 1990; Murff 1994; Houlsby and Martin 1992; Bransby and Randolph 1998; Mayne et al. 1995). Plasticity methods have been used to formulate yield loci for combined loading response. Empirically fitted yield loci based on centrifuge or 1 g model tests have also been proposed (Martin 1994; Murff 1994; Dean et al. 1992). Caisson (aspect ratio, L_f/D = 1) and spudcan response in normally consolidated clay was studied by Cassidy and Byrne (2001) and Cassidy (2012) using the drum centrifuge at the University of Western Australia. Martin (2001) investigated the vertical bearing capacity of shallow skirted foundations using lower and upper bounds of plasticity and presented results of a parametric study in the form of dimensionless charts, which compared well with findings by Villalobos et al. (2009).

Failure envelopes have been studied in detail for caissons with aspect ratios (L_f/D) of 1 (Gourvenec 2007; Gourvenec 2008) and 5 (Zhang et al. 2011; Lau 2015) based on both centrifuge tests and finite element results. The ultimate capacity under monotonic load for aspect ratio of 5 was found to be comparable to calculations based on existing design methods, including empirical methods and theoretical plasticity solutions (Zhang et al. 2011).

The complex interaction of vertical, horizontal and moment loads is further influenced by a dependence on soil strength profile. The analysis by Randolph (Randolph and Houlsby 1984) is also relevant to the vertical insertion or extraction of a T-bar penetrometer (Stewart and Randolph 1991) which was used to characterize strength in these experiments.

EXPERIMENTAL MODEL

Centrifuge testing was carried out at the Center for Earthquake Engineering Simulations facility at Rensselaer Polytechnic Institute (Elgamal et al. 1991). Loads were applied on the model foundations using the 4-degree of freedom in-flight robot fitted with a customized adaptor designed to be used with two different types of pile caps to achieve both pinned and rigid connections (Figure 1). These connectors transferring the load onto the pile were designed and fabricated to accommodate both rotation and translation motions.

A metal sphere on the top of the pile cap and a cylindrical socket on the adaptor fitted together forming a ball and socket joint allowing the pile to rotate freely (Figure 2 a). This pinned connection was designed to apply horizontal load with four different eccentricities, $e = 1.25D$, $1.5D$, $2.5D$ and $3.5D$. Eccentricity here is defined as the distance between the point of application of load and the mudline. The translation connector had a flat plate on the pile cap which fit into a groove in the adapter providing a rigid locking connection (Figure 2 b).

The model piles were fabricated from hollow aluminum tubes (Young's modulus, E_p = 70 GPa). Using the appropriate scaling laws (Murff 1996) these model piles had the following dimensions: outer diameter of 49.6 mm (3.72 m in prototype scale, for the test acceleration of 75 g); thickness of 0.609 mm (0.045 m in prototype scale); and effective embedment length of 101.6 mm (7.62 m in prototype scale). Rubber coating was applied on the model piles to protect the strain gauges and wires from water and soil particles. At 75 g the flexural rigidity of this hollow model pile was equal to 31.2 GNm^2. By assuming Young's modulus of steel as 200 GPa, this model pile is equivalent to a hollow steel pile with a diameter of 4 m and thickness of 12.5 mm in the field.

Linear Variable Displacement Transducers (LVDT) measured displacement of each pile using a steel bracket mounted on the edge of the rigid box (Figures 3 and 4). The stems of the connectors were strain gauged to measure the applied vertical and horizontal forces. Single dimensional Memsic 10 g accelerometers based on microelectromechanical systems (MEMS) were mounted on the model foundations with a 3D printed platform to measure tilt (Figure 2). A 100g MEMS accelerometer clamped on a 3D printed skirted mud mat foundation was placed in the test bed (Figure 3) at the height of the other MEMS accelerometers to measure the exact gravity (g) level required for measuring tilt (Beemer et al. 2017a).

The model construction consisted of four main parts: soil placement, consolidation, excavation and pile installation. Two soil layers formed the test bed were; a layer of Nevada sand (1 cm thick) and a layer of kaolinite (32 cm thick). The kaolin (Table 1) was mixed from dry powder at a water content of 77% and placed in three layers by hand. The test bed was constructed to be doubly drained and was consolidated in the centrifuge at 100g with a sand overburden layer. The degree of consolidation was controlled using the overburden pressure and spin time. Pore pressure sensors were placed within the clay bed to track the progress of consolidation. 40 kPa of pore pressure had to be dissipated at mid depth of the test bed (at 100 g) in order to simulate a shear strength profile similar to what is found on the seafloor. After completion of consolidation the upper overconsolidated layer was excavated. The final soil profile of the test bed after consolidation and excavation, consisted of a 20 cm (15 m in prototype scale, for the test acceleration of 75 g) thick layer of clay over a 1 cm (0.75 m in prototype scale) thick drainage layer of sand, with a 4 cm (3.0 m in prototype scale) freeboard of water. The model piles were installed with a spacing of 18.5 cm (center-to-center) along the center line of the spinning arm of the centrifuge (Figures 3 and 4), ensuring negligible boundary effects between the piles (Ullah et al. 2017). Details of model construction and consolidation are extensively described by Murali et al. (2015), Grajales et al.

(2015) and Beemer et al. (2016).

Strength Characterization

The shear strength of the clay bed was characterized in flight by using a T-bar penetrometer (Stewart and Randolph 1991) available at Rensselaer Polytechnic Institute (T-bar dimensions: 5 mm diameter and 20 mm length). A penetration rate of 2 mm/s was used to carry out the T-bar tests, which was consistent with the rate of pile loading tests and also provided undrained conditions in the kaolinite.

The T-bar penetrometer is now a widely used offshore site investigation tool with its primary advantage of profiling the undrained strength of soft clays (typically < 10 kPa) far better than other conventional tests (Randolph 2016). The T-bar makes use of the plasticity solution for the limiting pressure acting on a cylinder moving horizontally through a purely cohesive soil (Randolph and Houlsby 1984) based on a local flow around failure method. Numerical and theoretical solutions have been developed to determine appropriate N_{kt} factors for estimating undrained shear strength (Randolph 2004; Einav and Randolph 2005; Randolph and Andersen 2006; Martin and Randolph 2006; White et al. 2010). To compute the shear strength below a depth of 1.5 m, a T-bar factor, N_{kt} of 10.5 was used based on the existing research. A different failure mechanism (White et al. 2010) was used to compute the data from shallow depths. The T-bar data was also corrected for rate penetration effects based on Yafrate and DeJong (2007) and DeJong et al. (2011).

Figure 5 presents T-bar test results from a representative model test bed, complete strength profiles were presented by Murali et al. (2015) and Grajales et al. (2015). Multiple T-bar tests were carried out in each test bed spanning a time of approximately 2 hours, explaining the steady increase in average shear strength with every consecutive test (i.e. from T-bar test a through e), this is also shown in Figure 5. Until a depth of about 6 m below the mudline the strength profiles are uniform and at deeper sediments the strength gradually increases linearly. Multiple cores were also extracted along the test bed after completion of the test using a 1.9 cm (0.75 inch) hand sampler. The range of water content (minimum and maximum measured) values from these cores was used to compute the range of shear strength also presented in Figure 5 (Tessari 2012). There is good correlation between the estimated and measured shear strength profiles.

TESTING PROGRAM

The pile tests were carried out at a centrifugal acceleration of 75 g (at the pile mid-depth), in four different test beds. Eight different piles tests at different eccentricities (e/D = 0, 1.25, 1.5, 2.5 and 3.5) and different types of kinematic constraints (rotation and translation) are presented in this paper. Details are in Table 2. All the piles were pushed horizontally to large displacements (15 mm or 30% of the pile diameter) in order to obtain the ultimate horizontal capacity. Four of the piles were pushed to failure after a cyclic testing program of 50 - 200 cycles with varying displacement amplitudes. The effects of horizontal loading applied at different eccentricities on piles of aspect ratio of 2 was examined under monotonic loading conditions. All the tests were conducted under displacement control and a displacement rate of 2 mm/s.

The strength profile of the clay was obtained by carrying out a T-bar test before and after each pile test near every pile. Each pile test was normalized by the appropriate shear strength profile ensuring that the effects of strengthening of the clay bed through continued consolidation was removed. All the tests (pile tests and T-bar tests) in the same clay bed were carried out within a time span of approximately 2 hours (469 days in prototype time).

Even though no vertical displacement was formally applied in this test program, self weight of the pile and connectors simulated a constant vertical load, while the horizontal displacements and rotations were applied to reproduce the environmental loads on the foundation. Based on Martin (2001)'s vertical bearing capacity factors, for a pile with L_f/D of 2 and assuming a lower bound analysis for an adhesion factor, α of 0.7 in homogenous soil, approximately 55.35% of the total vertical bearing capacity was mobilized for pile with e = 1.25 (lowest vertical load) and 75.55% of the total vertical bearing capacity was mobilized for the pile with e = 2.5 (highest vertical load). Ratios V/V_{max} for each pile test are listed in Table 2.

FINITE ELEMENT MODEL

Model Geometry and Material Properties

A three dimensional finite element (FE) model was developed using Abaqus v6.12. The pile was considered to be a hollow and infinitely rigid structure (i.e. the soil inside the pile is taken into account) of 5 m diameter. An aspect ratio (L_f/D) of 2 was used to compare the FEM predictions with results obtained from the experimental model testing.

A cylinder of soil was used as the mesh configuration, with the pile embedded in the center (Figure 6). A number of geometric configurations were compared to maximize effectiveness of the model. The radial extent (center line to the far end of the cylinder) of the mesh is five diameters (5D) and the soil depth below the tip of the pile was set to be four times the diameter (4D). Elements adjacent to the pile were configured such that the ratio of the radial increment and circular segment were equal to one. The radial elements at the far ends used infinite elements to avoid any boundary effects.

The soil was assumed to be a single phase material, isotropic (i.e. undrained shear strength, s_u, is independent of the shearing mode and the type of load applied) and rate independent. The material model was assumed to be linear-elastic with Mohr-Coulomb plasticity which assumes an associated flow rule and a Mohr-Coulomb yield criterion. For this specific case, the yield criterion is the pressure independent Tresca model since the friction angle is set to zero (ϕ = 0). Hardening is permitted after yield conditions are reached. Undrained shear strength of the soil is assumed to increase with depth with a linear relationship given by s_u = 2.5 + 1.5z, where z is the depth in m and s_u is the undrained shear strength in kPa. This assumed strength profile is in agreement with experimental data and also lies within a range of typical marine clay strength profiles (Aubeny et al. 2001b).

Rigidity index, I_r, is defined as the ratio between the shear modulus (G) and the undrained shear strength (s_u). Vesic (1972) presented rigidity indices for soft to very stiff clays ranging from 10 to 300 respectively. Foott and Ladd (1981) published correlations of normalized secant modulus (E_u/s_u) against the shear stress ratio (τ_u/s_u) for a variety of clays. Using their data for marine clays, at τ_u/s_u = 50% the range of normalized secant moduli E_{50}/s_u is 300-600. An estimated range of rigidity indices I_r = 100-200 is produced for undrained loading on normally consolidated marine clays by assuming a poisson ratio of 0.5 (Aubeny and Grajales 2015). The finite element model however has been configured with a rigidity index of 50. While this value is somewhat low compared to the usual range of clayey soils, the strength of the soil bed in the experiments was very low.

Simulations are displacement controlled with a horizontal displacement applied to produce bearing failure of the soil. For cases in which translational displacement fields are needed, the pile is limited to move only in the direction of loading (i.e. torsion or rotation are not allowed). For simulation cases where the pile fails in rotation, no kinematic constraints are applied to the pile itself.

It has been reported that on comparing finite element analyses with either laboratory data, field data or exact solutions, FEM analyses tends to overestimate results. This is possibly related to the fact that finite element models create high stress concentrations around the pile tip (Aubeny et al. 2001a; Aubeny et al. 2003). To account for this high stress concentration the tip of the pile includes reduced strength elements.

While the formation of gaps is a common phenomenon observed on horizontally loaded piles in clay soils, gapping will not be addressed in this paper. Furthermore, assuming full contact at the pile-soil interface allows comparison of predicted values with exact solutions, such as the one developed by Randolph and Houlsby (1984).

The finite element model used for this research has been calibrated using a number of solutions available in the literature (Grajales 2017). It was configured in such a way that when analyzing plane strain conditions (i.e. deep enough depths such that surface effects can be neglected and the soil is flowing around the pile) exact agreement is found with solutions published by Randolph and Houlsby (1984).

RESULTS AND DISCUSSION

Translational response

The force-deflection curve for the pile tested in translation is presented in Figure 7 along with the finite element results and computed ultimate horizontal capacity using methods proposed by Murff and Hamilton (1993). The horizontal head load, H, is presented as a horizontal bearing factor N_h, which is obtained normalizing by the average shear strength $s_{u,avg}$ over the depth of pile embedded in soil and the product of the projected vertical area, $L_f D$. For experimental data, the maximum value measured is defined as the ultimate capacity.

In the experiments, the pile was displaced horizontally to an amplitude equal to $0.3D$ (30% of the pile diameter). The total displacement experienced by the pile was a combination of translation with a component of rotation (2.7 degrees), measured using the displacement and tilt sensor respectively. The effect of this tilt on the ultimate capacity of the pile was found to be negligible as it developed due to compliance between the pile cap and the adaptor as the pile was horizontally loaded. For clarity in presentation, the horizontal bearing factor is plotted against normalized displacement at the center of rotation for the pile. The pile appears to reach its maximum value at approximately $0.1D$ displacement amplitude, with the calculated horizontal bearing capacity factor (N_h) being approximately equal to 9.9.

Ultimate horizontal capacity of the pile tested in translation is found to be in the middle of the range of values predicted by Murff and Hamilton (1993) upper bound solution for no gapping. The horizontal gray shaded band in Figure 7 covers the range of adhesion between soil and pile from a low bearing factor of 8.95 for the smooth pile ($\alpha = 0$) to a bearing factor of 11.6 for rough pile ($\alpha = 1$). This result suggests that there was a fair amount of adhesion between the model pile and the soil.

Finite element results are presented for different adhesion factors α ranging from 0 to 1 obtaining horizontal bearing factors N_h of 8.08 and 10.8 respectively. Also comparable in the plot is the stiffness of the experimental data and the finite element results that model the pile as a rigid structure.

Maximum capacity ($N_h = 9.9$) occurs at a displacement y/D of approximately 10%. These results match fairly well with finite element predictions for an adhesion factor $\alpha = 0.67$ (horizontal bearing factor N_h of 10). Once again, this suggests that adhesion existed between the model pile and soil. The most probable cause for this behavior is the fact that model piles were rubber coated in order to protect strain gages and wires from water and soil particles (see Figure 2).

Despite the fact that the formation of gaps behind horizontally loaded piles is a phenomenon that has been observed by several researchers (Zhang et al. 2011), testing accommodations did not allow a high speed camera to be mounted inside the bucket during the spin. Therefore, no evidence of gapping was observed.

Rotational response

The monotonic response of a pile subject to rotation was investigated for horizontal loads applied at four different eccentricities (e): 1.25D, 1.5D, 2.5D and 3.5D. The horizontal load, H, was normalized by the average shear strength profile over the depth of pile embedment, $s_{u,avg}$ and the product of the projected vertical area, $L_f D$. The horizontal displacement, y, was computed at the mudline using the tilt and displacement measurements and normalized by the pile diameter, D. All the piles were pushed horizontally at the top of the ball and socket connector to a displacement amplitude equal to $0.3D$. Thus the final pile displacement amplitude at the mudline varied depending on the eccentricity. Results for these tests are presented in Figure 8 (a) through (d). Force displacement curves are plotted for both cases of primary loading (red circles) and post-cyclic loading (blue squares). Finite element predictions for adhesion factors ranging from 0 (smooth interface) to 1 (rough interface) are plotted along experimental results for each of the eccentricities studied.

As might be expected, horizontal capacity is inversely proportional to eccentricity (i.e. capacity decreases with increasing eccentricity) for both primary and post-cyclic monotonic loading. Another important observation is what appears to be a work hardening behavior in all of the rotation tests indicating that the piles mobilize increasing strength with increasing displacements due to the rotational failure mechanism of short aspect ratio piles. This behavior has been previously reported by several authors (Lau 2015; Zhu et al. 2015).

One of the discrepancies between finite element results and experimental data is the slope of the load-displacement curves. Finite element results appeared to be less stiff in the case of rotational displacement fields, except for Figure 8 (d), in which the experimental data seems to fall within the predicted range.

For the case of eccentricity, $e = 1.25$ (Figure 8a), experimental data show that capacity keeps increasing even after a displacement of $0.1D$ (at the top of the pile). However, if a serviceability limit of $0.05D$ is assumed, results for both primary and post-cyclic loading tests seem to fall into the range predicted by finite element simulations. From experimental data, horizontal bearing factors N_h of approximately 1.4 and 1.46 are obtained for primary and post-cyclic loading respectively, while finite element predictions for an adhesion factor (α) of 0.67 seem to be around 1.45.

For the cases of eccentricities, $e = 1.5D$ and $e = 2.5D$, both experimental and numerical results are in reasonable agreement up to a normalized displacement of $0.1D$. From Figure 8(b) it is observed that, at 5% displacement, experimental results seem to be within the range of values encompassed by finite element predictions for adhesions $\alpha = 0.33$ and $\alpha = 0.67$ (i.e. horizontal bearing factors, N_h ranging between 1.1 and 1.35). On the other hand, for eccentricity, $e = 2.5D$ (Figure 8c), it appears that primary loading data is in agreement with finite element results for an adhesion of 0.67 while post-cyclic is approximately equal those of $\alpha = 0.33$. Experimental results are presented in tabular form at Table 3.

Finally, for eccentricity, e of 3.5 (Figure 8d) experimental data is in agreement with low adhesion finite element predictions up until y/D of 0.05.

Based on the results it appears that the experimental data is in overall agreement with the finite element predictions for adhesions between 0.33 to 0.67. The discrepancies in bearing factors between the experimental and the upper bound plastic limit analysis results are thought to be due to a combination of reasons. A major contributing factor is thought to be the combined effect of vertical and moment loading. There was also uncertainty on whether or not a gap developed at the back of the pile.

Another observation made during the testing was settlement of the piles during loading. The connectors did not constrain the pile vertically, thus as each pile was horizontally loaded there was a corresponding vertical settlement. The influence of this vertical settlement on the failure mechanism is explained briefly in Murali (2015). This paper does not examine the vertical settlement in detail due to insufficient measured data.

Effect of Eccentricity

A parametric study was developed using Aubeny et al. (2003) simplified plasticity method in order to assess the effect of eccentricity and compare it with existing solutions. A horizontal displacement was applied assuming the load attachment point to be ranging from well above the soil surface (around 5 diameters), to a distance equal to 3 diameters below the surface. This type of study has been typically developed to determine the optimal load attachment depth on suction anchors. Results are presented in Figure 9. Analytical predictions are presented for three different adhesions, α = 0, 0.67 and 1. Note that a negative sign denotes a load attachment point (i.e. eccentricity) above the soil surface.

As it was mentioned in the previous section, experimental results seem to be in agreement with predictions for adhesions $\alpha = 0.33$ and $\alpha = 0.67$. This indicates that upper bound methods initially developed by Murff and Hamilton (1993) and later improved by Aubeny et al. (2001a) and Aubeny et al. (2003) are predicting horizontal capacities comparable to the measured values. It is also important to remember that failure displacement level for experimental data was selected as 0.05D.

Finally, the result obtained from the pure translation test, is plotted at the location at which the maximum predicted capacity occurs. Once more, it appears that the experimental data falls closer to an adhesion of 0.67.

Center of rotation

The short rigid pile rotates about a point without flexing significantly. The variation of the center of rotation as the pile undergoes lateral loading is presented in Figures 10 and 11 for primary loading and post cyclic loading respectively. The mudline and the bottom of the pile are indicated in the figures.

Both figures show that the center of rotation drops below the base of the pile but quickly stabilizes at a depth ranging between the pile mid-depth and the pile base. Also observed in Figures 10 and 11 is that the center of rotation moves deeper below the mudline and closer to the pile base with increase in eccentricity. This suggests that differing aspect ratio (applicable only to short rigid piles) might not influence the center of rotation as much as change in eccentricity or point of loading. The center of rotation also stabilizes much faster with decreasing eccentricity suggesting that the tip failure mechanism consisting of a spherical failure surface (Aubeny et al. 2001a) occurs earlier or at a lower normalized displacement for the piles at lower eccentricity.

Vertical-Horizontal Load Interaction

It is clear from the experimental results that the assessment of failure is subjective and a systematic approach is required to correlate the results from the different tests. The yield points for analysis are determined by selecting bearing factors for all the tests corresponding to a $0.05D$ displacement.

A simplified upper bound solution presented by Aubeny et al. (2003) has been utilized to develop an interaction diagram somewhat similar to the ones presented by Aubeny et al. (2003) and Clukey et al. (2004). Figure 12 shows horizontal and vertical resistance normalized by the maximum capacity for cases of pure axial and lateral translation respectively (i.e. $N_v = 12.3$ and $N_h = 10.96$, both computed using Aubeny et al. (2003) method). Experimental data points were computed based on the data reported in Tables 2 and 3. In general, a fair agreement is observed between analytical predictions and measured data.

A first observation on Figure 12 is that the self weight of the model piles represents a fairly heavy structure. All data points show that there is more than 50% of vertical capacity is mobilized in all of the tests conducted. It is likely that the failure mechanism developed by model piles during centrifuge testing is dominated by vertical loading instead of horizontal, as evidenced by the low horizontal load mobilized at failure, ranging from 0.075 to 0.16 H_{max}.

Analytical predictions seem to fall slightly above data points. This suggests that the simplified upper bound solution is slightly un-conservative. The amount of over-prediction increases with eccentricity. This observation is consistent with the observation that plasticity methods tend to over-predict capacities for short piles, mostly for cases in which the load application point is above the mudline.

Moment-Tilt Curves

The moment-tilt curves for all of the piles tested in rotation is presented in Figures 13a (primary loading) and 13b (post cyclic loading). The moment, M, is computed at the mudline for comparison of piles tested at different eccentricities and normalized by $L_f^2 D$ and the average shear strength profile $s_{u,avg}$ along the pile embedment. The pile tilt or degree of rotation from the vertical axis, θ, is computed using the MEMS sensors (Beemer et al. 2017b).

The moment at the mudline increases with increase in eccentricity as expected. Achmus et al. (2009) developed a stiffness degradation model for offshore wind towers based on finite element simulations and an experimental evaluation of drained cyclic triaxial tests on a sandy seabed. They reported a maximum tolerance of 0.5^o of permanent tilt at the mudline. All the tests carried out in this research program all failed at very low tilt angles ($< 2^o$). Although Achmus et al. (2009) studied permanent tilt and not static capacity tilt, loading the structure beyond the elastic tilt range (or $> \theta_f$) leads to a permanent tilt. The allowable elastic tilt range is found to be very low for these piles which is an important design consideration.

All of the piles were installed by hand in 1 g conditions and the centrifuge spun up to reach the test acceleration. Table 4 presents the initial tilt measured by the MEMS sensor at 1 g ($\theta_{in,1g}$) at the time of installation and the tilt after spin up at 75g ($\theta_{in,75g}$) for all the primary monotonic tests. The initial tilt data is not applicable to the post cyclic monotonic tests. The maximum tilt developed during spin up appears to be for pile P1 with a $\Delta\theta_{spinup}$ of 1^o. Based on the results of repeat pile tests in different soil beds, the initial tilt developed during spin up is not assumed to influence the ultimate capacity results.

CONCLUDING REMARKS

Behavior of short piles and caissons has been studied by means of geotechnical centrifuge and numerical analyses. The main aspect discussed in this article is capacity for both translational and rotational displacement fields. For the latter, four different eccentricities were considered: e/D = 1.25, 1.5, 2.5 and 3.5. The following remarks are concluded:

- Ultimate capacity in translation corresponds to a bearing factor of 9.9 (Figure 7). This result compares well with the finite element prediction using an adhesion factor of 0.67. The rubber coating applied to the model piles used in this study is thought to contribute to the adhesion. There is also significant comparison in the ”stiffness” (i.e. slope of the load-displacement curve) from experimental data and finite element results that models the pile as a rigid body.
- Predictions using the full upper bound plasticity solution proposed by Murff and Hamilton (1993) over-predicts capacities for short piles and caissons. However the simplified upper bound solution by Aubeny et al. (2003) is more accurate. An accurate description of the failure mechanisms is needed to capture the real behavior of these short piles.
- The rotational capacities of model piles were found to be comparable to the values predicted by finite element simulations with no gapping. Given the work hardening behavior observed during the tests, and based on the fact that both the finite element model and plasticity solutions are developed for small strains, a displacement level of 5% of the pile diameter (at the top of the pile) was selected as the failure criterion. Selection of a serviceability criterion is dependent on the type of structure.

Vertical settlement was visually observed (with limited measurement) on all the pile tests to varying levels and more research is required to obtain a deeper understanding on the failure mechanism of short aspect ratio piles. Although vertical settlement was not foreseen, it actually resembles real field conditions, in which the weight of the structure also affects the failure mechanism of the foundation system. Mobilized vertical capacities of above 50% were found. Examination of horizontal capacity ratios suggests that the failure mechanism developed by the model piles is fundamentally controlled by vertical loads instead of horizontal ones. Future centrifuge model testing should ideally be carried out without restricting vertical settlement of the pile to obtain behavior that would simulate field conditions.

Further studies are required to develop a complete understanding of the behavior of short piles. Aspects such as the hardening occurring on moment-tilt curves, quantification of skin friction and the effect of vertical load and settlement should be addressed in future experiments. Finally, characterization of gapping is also needed.

ACKNOWLEDGEMENTS

The authors would like to acknowledge support from the National Science Foundation for the project *Capacity and Performance of Foundations for Offshore Wind Towers*, Award Number: 1041604. Additionally we would like to acknowledge the NEES site and their personnel at Rensselaer Polytechnic Institute.

REFERENCES

Achmus, M., Kuo, Y., and Abdel-Rahman, K. (2009). "Behavior of monopile foundations under cyclic lateral load." *Computers and Geotechnics*, 35 (5), 725–735.

Andersen, K., Murff, J., Randolph, M., Clukey, E., Erbrich, C., Jostad, H., Hansen, B., Aubeny, C., Sharma, P., and Supachawarote, C. (2005). "Suction anchors for deepwater applications. keynote lecture." *Proceedings of the International Symposium on Frontiers in Offshore Geotechnics, Perth, Western Australia.* (September).

Aubeny, C. and Grajales, F. (2015). "Strain path analysis of setup time around piles and caissons." *Proceedings of the ASME2015 34 Int. Conf Ocean, Offshore and Arctic Engr, OMAE2015*.

Aubeny, C., Han, S., and Murff, J. (2003). "Inclined load capacity of suction caissons." *Int. J. Numer. Anal. Meth. Geomech.*, 27, 1235–1254.

Aubeny, C., Moon, S., and Murff, J. (2001a). "Lateral undrained resistance of suction caisson anchors." *Intl. J. Offshore and Polar Engineering*, 11 (3), 211–219.

Aubeny, C., Murff, J., and Roesset, J. (2001b). "Geotechnical issues in deep and ultra deep waters." *The International Journal of Geomechanics*, 1, 225–247.

Beemer, R., Murali, M., Aubeny, C., and Biscontin, G. (2016). "Rotational behavior of squat monopiles in soft clay from centrifuge experiments." *Conference paper under review: GeoChicago2016*.

Beemer, R. D., Aubeny, C., and Biscontin, G. (2017a). "Centrifuge 2d gravity on a vertical rotational reference frame." *International Journal of Physical Modelling in Geotechnics (In Press)*.

Beemer, R. D., Murali, M., Aubeny, C. P., and Biscontin, G. (2017b). "Use of a mems accelerometer to measure orientation in a geotechnical centrifuge.." *International Journal of Physical Modelling in Geotechnics (In Press)*.

Bransby, M. F. and Randolph, M. (1998). "Combined loading of skirted foundations." *Géotechnique*, 48 (5), 637–655.

Cassidy, M. (2012). "Experimental observations of the penetration of spudcan footings in silt." *Geotechnique*, 62(8), 727–732.

Cassidy, M. and Byrne, B. (2001). "Drum centrifuge model tests comparing the performance of sspudcan and caissons in kaolin clay." *Report No. Report No. OUEL 2248/01*, University of Oxford.

Clukey, E., Aubeny, C., and Murff, J. (2004). "Comparison of analytical and centrifuge model tests for suction caissons subjected to combined loads." *Journal for Offshore Mechanics and Arctic Engineering, ASME*, 126 No. 4, 364–367.

Dean, E. R., James, R., Schofield, A. N., Tan, F., and Tsukamoto, Y. (1992). "The bearing capacity of conical footings on sand in relation to the behaviour of spudcan footing of jackups." *Proceedings of the Wroth Memorial Symposium 'Predictive soil mechanics'*, 230–253.

DeJong, J. T., Yafrate, N. J., and DeGroot, D. J. (2011). "Evaluation of undrained shear strength using full-flow penetrometers." *Journal of Geotechnical and Geoenvironmental Engineering*, 137 (1), 14–26.

Einav, I. and Randolph, M. F. (2005). "Combing upper bound and strain path methods for evaluating penetration resistance." *Int. J. Numer. Methods Eng.*, 63(14), 1991–2016.

Elgamal, A., Dobry, R., and Van Laak, P. (1991). "Design, construction and operation of 100 g-ton centrifuge at rpi." *Centrifuge*, Boulder, CO, 27–34.

Foott, R., R. and Ladd, C. (1981). "Undrained settlement of plastic and organic clays." *Journal of the Geotechnical Eng Division, ASCE*, 107(GTS), 1079–1094 Proc. Paper 16421.

Garnier, J. and Gaudin, C. (2007). "Catalogue of scaling laws and similitude questions in centrifuge modelling. International Technical Committee TC2 (Physical Modelling in Geotechnics, PMG).

Gourvenec, S. (2007). "Failure envelopes for offshore shallow foundations under general loading." *Géotechnique*, 57 (9), 715–727.

Gourvenec, S. (2008). "Effect of embedment on the undrained capacity of shallow foundations under general loading." *Geotechnique*, 58(3), 177–185.

Grajales, F. (2017). "Lateral capacity of piles and caissons in cohesive soils." phdthesis, phdthesis.

Grajales, F., Beemer, R. D., Murali, M., Aubeny, C., and Biscontin, G. (2015). "Response of short monopiles for offshore wind turbine foundations: virgin and post-cyclic capacity.." *Proceedings of the 68th Canadian Geotechnical Conference, Quebec, CA*.

Hamilton, J., Phillips, R., Dunnavant, T., and Murff, J. (1991). "Centrifuge study of laterally loaded piles in soft clay." *Proc Int Conf Centrifuge 1991, ISSMFE.*

Houlsby, G. T. and Martin, C. M. (1992). "Modelling of the behaviour of foundations of jack up units on clay.." *Proceedings of the Wroth Memorial Symposium 'Predictive soil mechanics'*, 339–358.

Jeanjean, P. (2009). "Re-assessment of p-y curves for soft clays from centrifuge testing and finite element modeling." *Proc. Offshore Technology Conf., Paper OTC20158, Houston.*

Lau, B. (2015). "Cyclic behaviour of monopile foundations for offshore wind turbines in clay." Ph.D. thesis, Ph.D. thesis.

Martin, C. M. (1994). "Physical and numerical modelling of offshore foundations under combined load." Ph.D. thesis, Ph.D. thesis.

Martin, C. M. (2001). "Vertical bearing capacity of skirted circular foundations on tresca soil." *Proc. 15th Int. Conference on Soil Mechanics and Geotechnical Engineering, Istanbul*, 743–746.

Martin, C. M. and Randolph, M. F. (2006). "Upper bound analysis of lateral pile capacity in cohesive soil..” *Geotechnique*, 56(2), 141–145.

Matlock, H. (1970). “Correlations for design of laterally loaded piles in soft clay.” *Proc. Offshore Technology Conference, OTC 1204, Houston.*

Mayne, P. W., Kulhawy, F. H., and Trautmann, C. H. (1995). “Laboratory modeling of laterally-loaded drilled shafts in clay.” *Journal of Geotechnical Engineering*, 121(12), 827–835.

Murali, M. (2015). “Characterization of soft clays and the response of soil-foundations systems for offshore applications.” Ph.D. thesis, Ph.D. thesis.

Murali, M., Grajales, F., Beemer, R., Biscontin, G., and Aubeny, C. (2015). “Centrifuge and numerical modeling of monopiles for offshore wind towers in clay.” *Proceedings of the 34rd International Conference on Ocean, Offshore and Arctic Engineering (OMAE2015-41332).*

Murff, J. (1996). “The geotechnical centrifuge in offshore engineering.” *Offshore Technology Conference (OTC8265), Houston, Tx.*

Murff, J. and Hamilton, J. (1993). “P-ultimate for undrained analysis of laterally loaded piles..” *ASCE Journal of Geotechnical Engineering*, 119 (1), 91–107.

Murff, J. D. (1994). “Limit analysis of multi footing foundation systems.” *Proc. 8th International conference of computational methods and advanced geomechanics.*, 223–244.

Palix, E., Willems, T., and Kay, S. (2011). “Caisson capacity in clay: Vhm resistance envelope - part 1: 3d fem numerical study.” *Frontiers in Offshore Geotechnics II - Gourvenec and White (eds).*

Pokrovsky, G. and Fyodorov, I. (1936). “Studies of soil pressures and ddeformation by means of a centrifuge..” *Proceedings of the 1st International Conference on Soil Mechanics and Foundation Engineering, Harvard, Cambridge, MA, 70.*

Randolph, M. F. (2004). “Characterisation of soft sediments for offshore applications.” *Proc. 2nd Int. Conf. on Site Characterisation, Millpress, Rotterdam, Netherlands*, 209–231.

Randolph, M. F. (2016). “New tools and directions in offshore site investigation.

Randolph, M. F. and Andersen, K. H. (2006). “Numerical analysis t-bar penetration in soft clay.” *Int. J. Geomech.*, 6(6), 411–420.

Randolph, M. F. and Houlsby, G. T. (1984). "The limiting pressure on a circular pile loaded laterally in cohesive soil." *Géotechnique*, 34(4), 613–623.

Reese, L. C., Cox, W. R., and Koop, F. (1975). "Field testing and analysis of laterally loaded piles in stiff clay." *Proceedings, Offshore Technology Conference, OTC 2312, Houston, Texas*, 671–690.

Stewart, D. P. and Randolph, M. F. (1991). "A new site investigation tool for the centrifuge." *Proc. Int. Conf. On Centrifuge Modelling, Balkema, Rotterdam, Netherlands*, 531–538.

Supachawarote, C., Randolph, M., and Gourvenec, S. (2004). "Inclined pull out capacity of suction caissons." *Proc. Fourtheenth Int. Offshore and Polar Engineering Conference, ISOPE*.

Tan, F. (1990). "Centrifuge and theoretical modelling of conical footings on sand." Ph.D. thesis, University of Cambridge, University of Cambridge.

Taylor, R. N. (ed.) (1995). *Geotechnical Centrifuge Technology*. CRC, London.

Tessari, A. (2012). "Centrifuge modeling of the effects of natural hazards on pile-founded concrete floodwalls." Ph.D. thesis, Rensselaer Polytechnic Institute, Rensselaer Polytechnic Institute.

Tjelta, T. (2001). "Suction piles: their position and applications today." *Proceedings of the 11th International Offshore and Polar Engineering Conference, Stavanger, Norway, June 17-22, Vol 2*.

Ullah, S. N., Hu, Y., Stanier, S., and White, D. (2017). "Lateral boundary effects in centrifuge foundation tests." *International Journal of Physical Modelling in Geotechnics*, 17, Issue 3, 144–160.

Vesic, A. (1972). "Expansion of cavities in infinite soil mass." *ASCE J. Geotech. Engng*, 98(3), 265–290.

Villalobos, F. A., Byrne, B. W., and Houlsby, G. (2009). "An experimental study of the drained capacity of suction caisson foundations under monotonic loading for offshore applications." *Soils and Foundations*, 49, No 3, 477–488.

White, D. J., Gaudin, C., Boylan, N., and Zhou, H. (2010). "Interpretation of t-bar penetrometer tests at shallow embedment and in very soft soils." *Can. Geotech. J.*, 47(2), 218–229.

Yafrate, N. J. and DeJong, J. T. (2007). "Influence of penetration rate on measured resistance with full-flow penetrometers in soft clay." *Proc., Advances in Measuring and Modeling of Soil Behavior, GeoDenver, Geotechnical Special Publication 173, ASCE.*

Yun, G. and Bransby, M. F. (2007). "The horizontal-moment capacity of embedded foundations in undrained soil." *Canadian Geotechnical Journal*, 44, 409–424.

Zhang, C., White, D., and Randolph, M. (2011). "Centrifuge modeling of the cyclic lateral response of a rigid pile in soft clay." *Journal of Geotechnical and Geoenvironmental Engineering*, 137(7), 717–729.

Zhu, B., Sun, Y., Chen, R., Guo, W., and Yang, Y. (2015). "Experimental and analytical models of laterally loaded rigid monopiles with hardening p-y curves." *Journal of Waterway, Port, Coastal and Ocean Engineering (ASCE)*, , 10.1061/(ASCE)WW.1943-5460.0000310 , 04015007.

NOTATION

The following symbols are used in this paper:

- D = pile diameter
- e = eccentricity (in diameters)
- E_u = secant modulus
- E_p = young's modulus
- H = horizontal load
- I_r = rigidity index
- L_o = center of rotation
- L_f = pile length
- N_h = horizontal bearing factor
- N_{kt} = T-bar bearing factor
- N_m = moment bearing factor
- N_p = equivalent horizontal bearing factor
- N_v = vertical bearing factor
- M = moment load
- s_u = undrained shear strength
- V = vertical load
- y = horizontal displacement
- z = depth
- α = adhesion factor, roughness
- θ = pile tilt
- τ = shear stress
- ϕ = friction angle

List of Tables

TABLE 1. Soil properties of kaolin used for testing

Property	Value
Manufacturer	BASF
Trade name	ASP 600
Specific gravity	2.64
Liquid limit	63
Plasticity index	33
Coefficient of consolidation, c_v ($m^2/year$)	0.51 - 0.90
Saturated unit weight, γ_{sat} (kN/m^3)	15.5
SHANSEP parameter, $(s_u/\sigma'_v)_{NC}$	0.22
SHANSEP parameter, m	0.8

TABLE 2. Test matrix

Test #	Movement	eccentricity e/D	Monotonic test	V/V_{max}
Test 1	translation	-	primary loading	0.335
Test 2	rotation	1.25	primary loading	0.553
Test 3	rotation	1.25	post cyclic loading	0.553
Test 4	rotation	1.5	primary loading	0.667
Test 5	rotation	1.5	post cyclic loading	0.667
Test 6	rotation	2.5	primary loading	0.755
Test 7	rotation	2.5	post cyclic loading	0.755
Test 8	rotation	3.5	post cyclic loading	0.687

TABLE 3. Normalized horizontal load and moment bearing factors

Pile test	e	N_h experimental	N_h - no gap (Aubeny et al. 2003)	N_m experimental
Test 2	1.25	1.4	1.58	0.87
Test 3	1.25	1.46	1.58	0.91
Test 4	1.5	1.22	1.45	0.92
Test 5	1.5	1.24	1.45	0.93
Test 6	2.5	0.99	1.09	1.24
Test 7	2.5	0.90	1.09	1.13
Test 8	3.5	0.65	0.87	1.14

TABLE 4. Tilt data for piles tested

Pile	e	$\theta_{in,1g}$	$\theta_{in,75g}$	$\Delta\theta_{spinup}$
Test 6	2.5	1.327	0.365	0.962
Test 4	1.5	-1.270	-1.940	0.670
Test 2	1.25	3.518	3.501	0.017

List of Figures

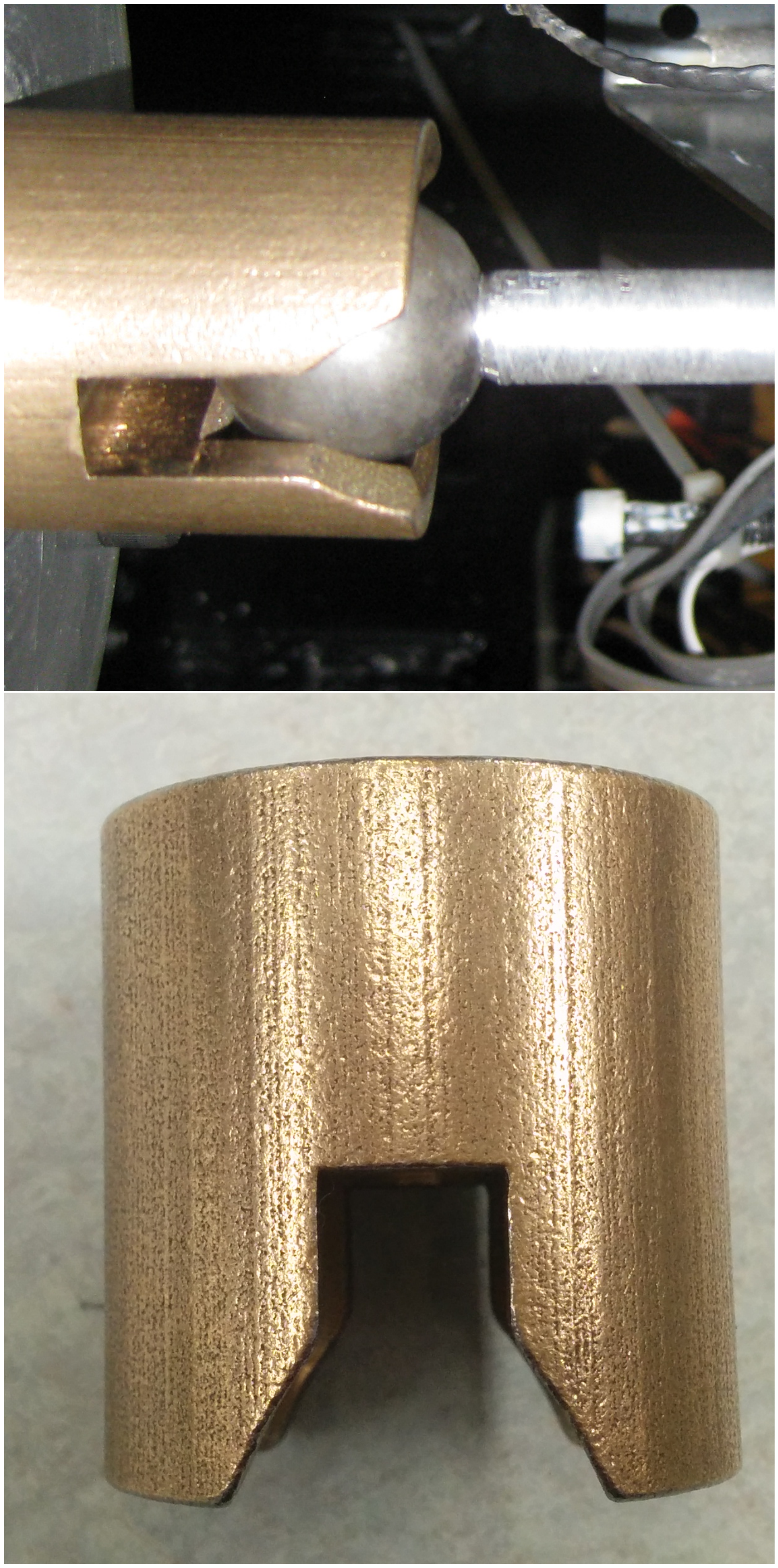

FIG. 1. Adaptor fitting along with pile load transfer connector.

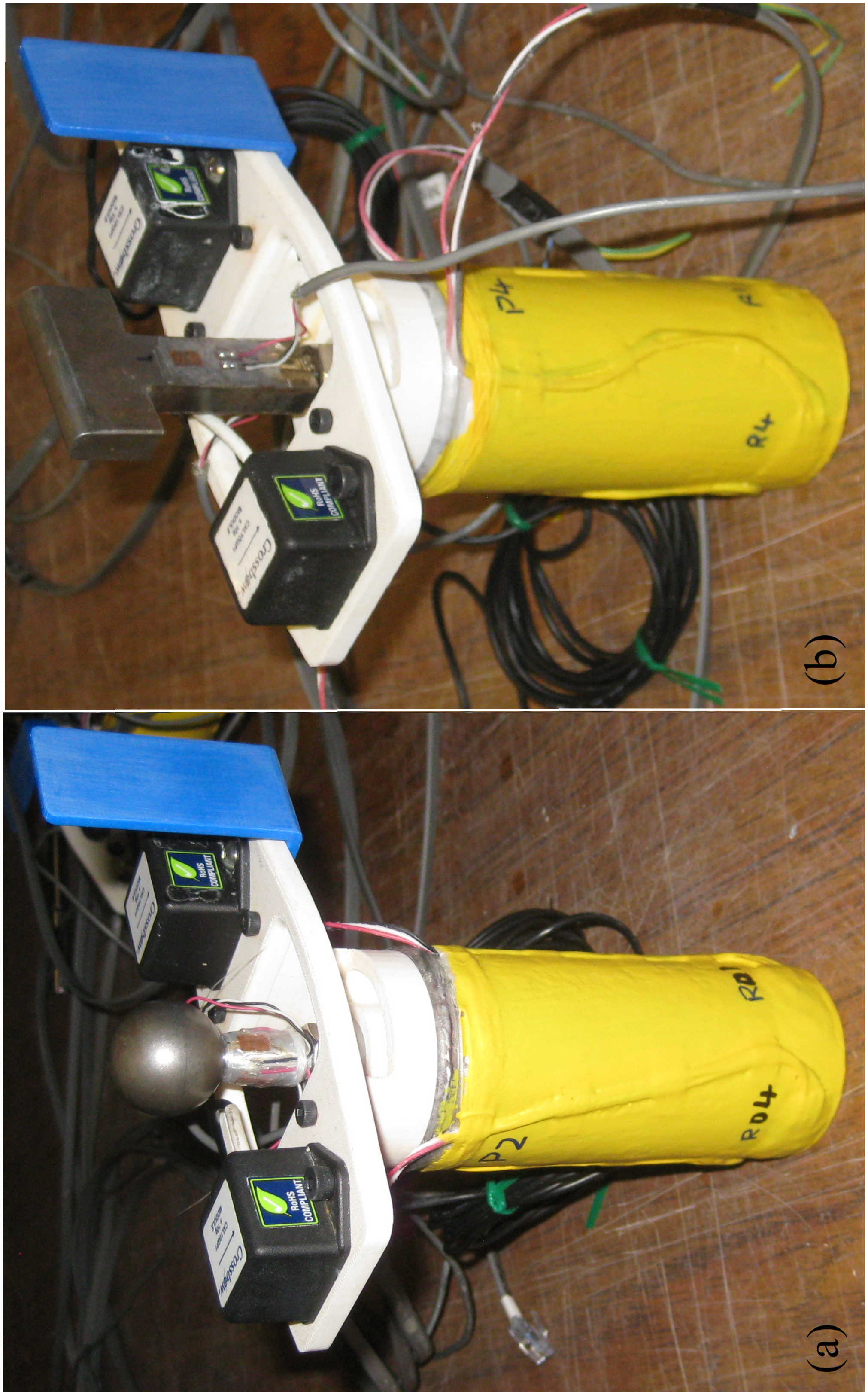

FIG. 2. a) Ball joint on pile to allow rotation ; b) Rigid connector on pile for pure translation.

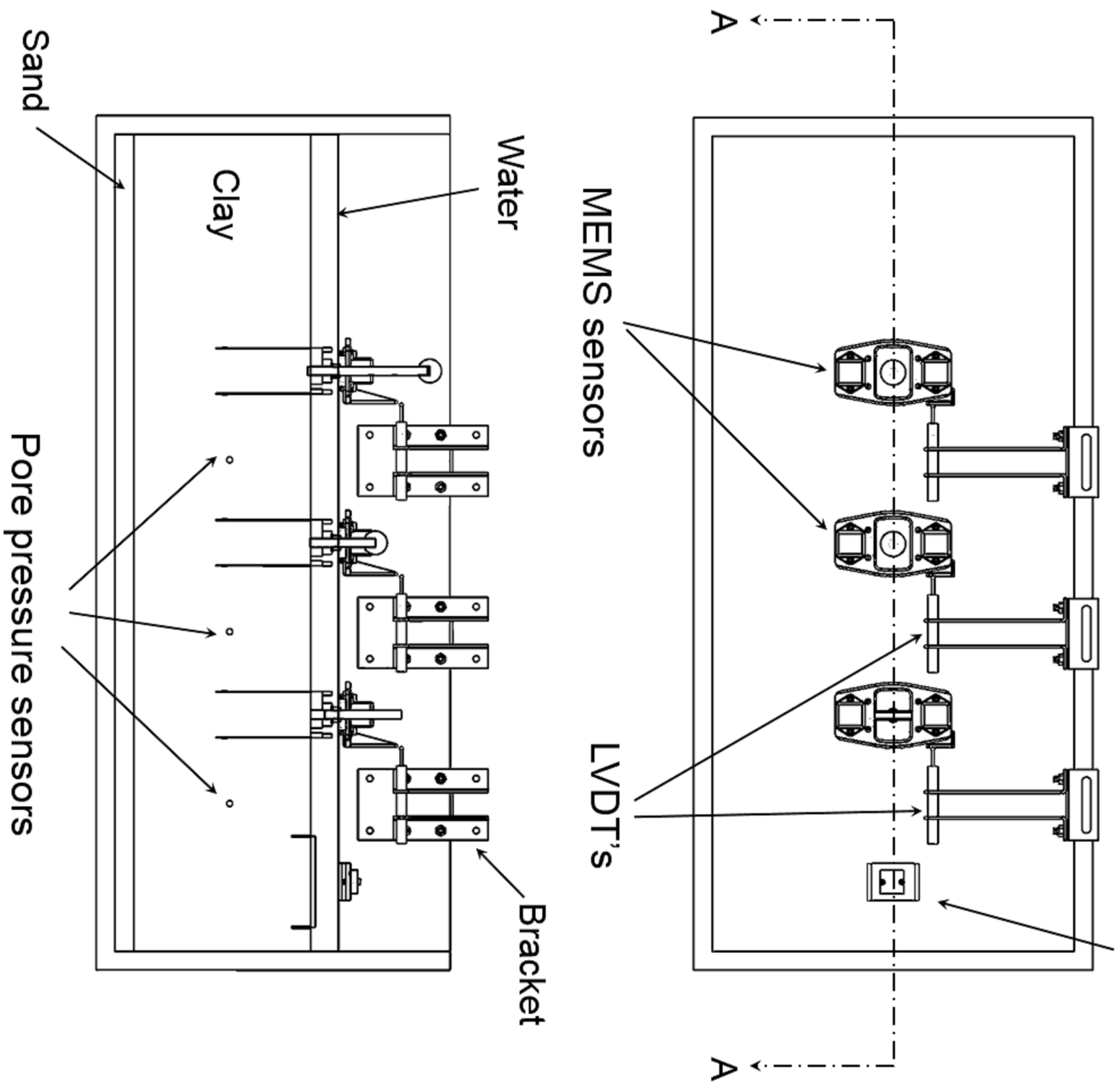

FIG. 3. Plan view (top) and section view (bottom) of the test arrangement. Picture to scale.

FIG. 4. Model testbed with piles installed.

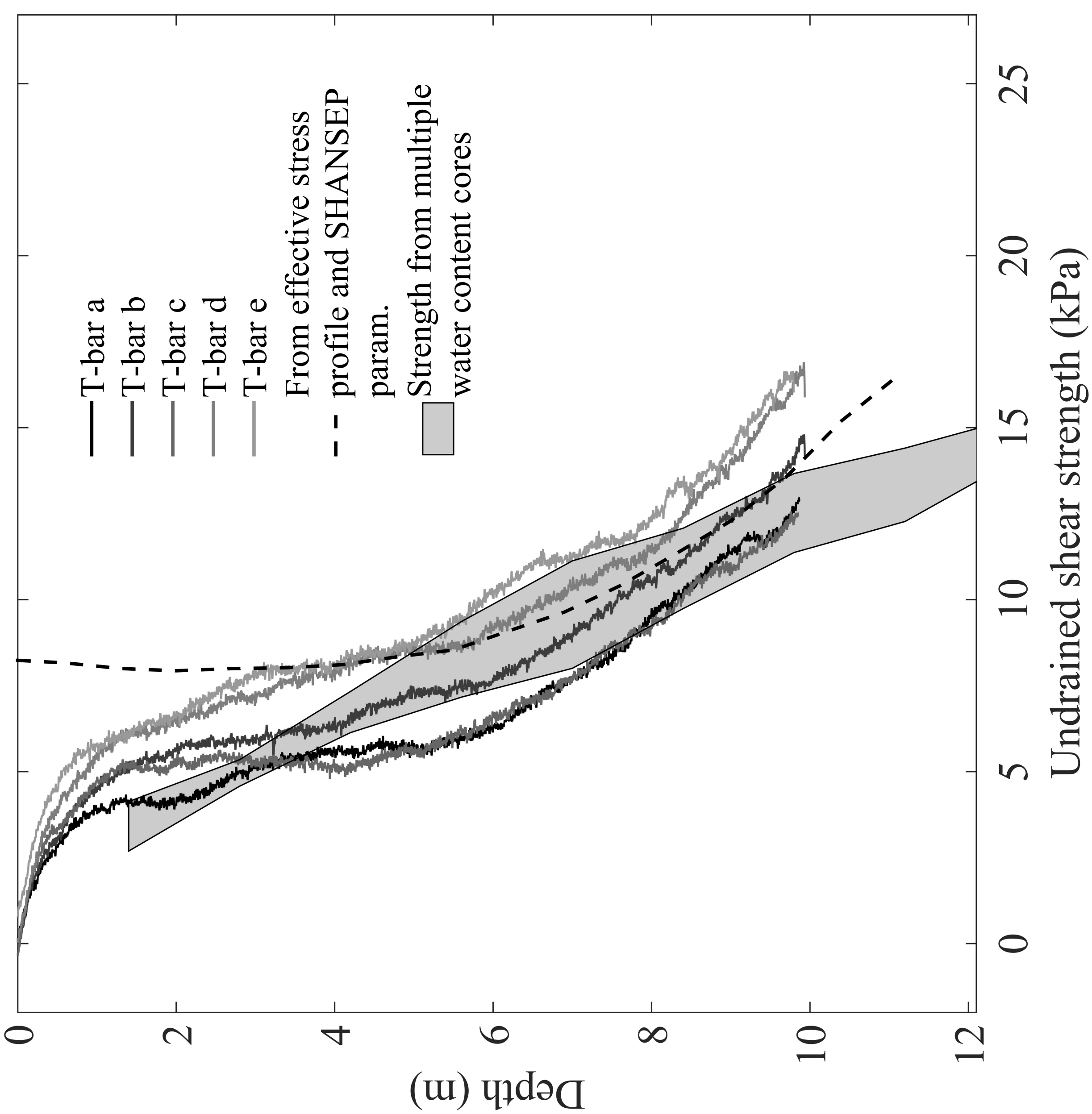

FIG. 5. Profiles for undrained shear strength for a representative test bed

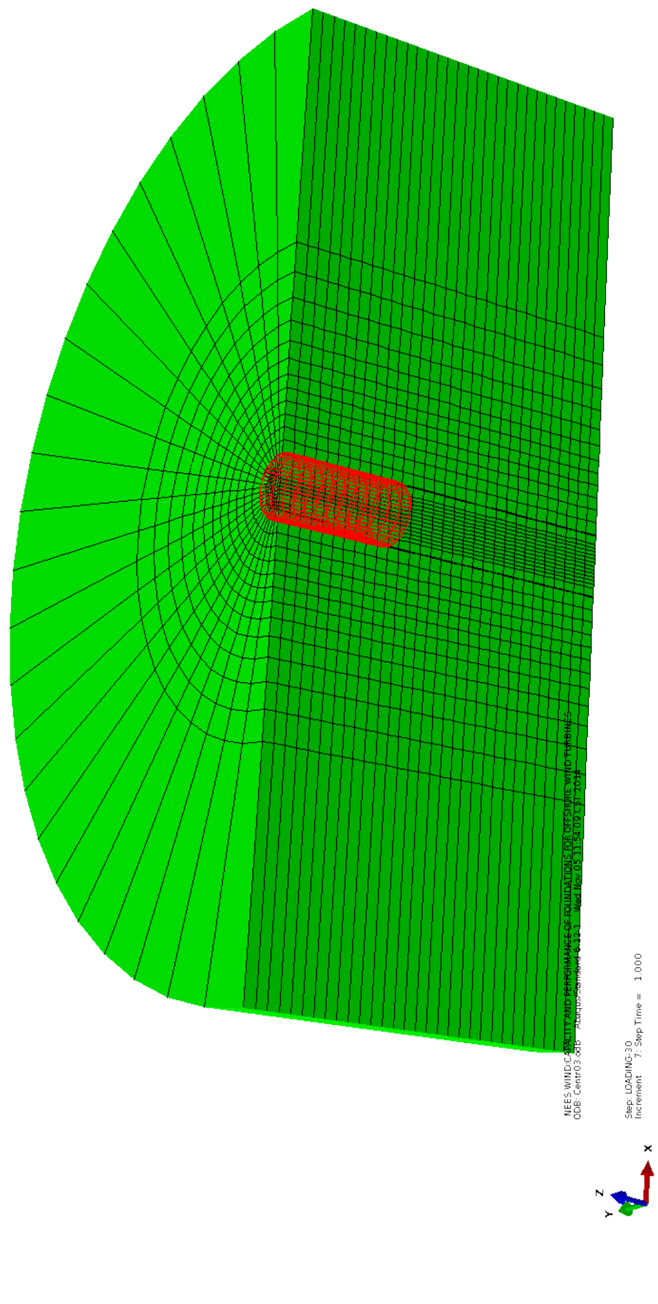

FIG. 6. Finite element mesh, undeformed configuration. (Note: Only half of the mesh is shown. The pile is highlighted in the middle)

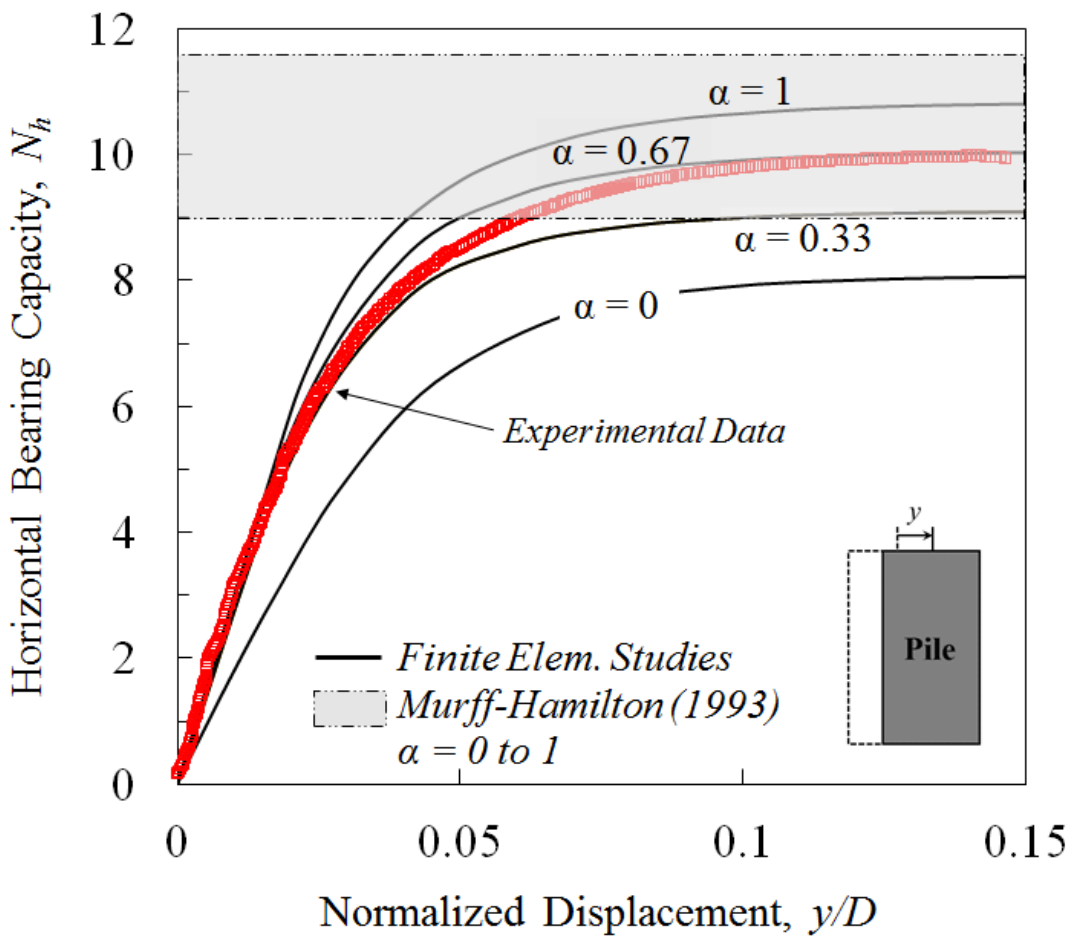

FIG. 7. Comparison of experimental results against finite element predictions and upper bound solutions (Murff and Hamilton 1993).

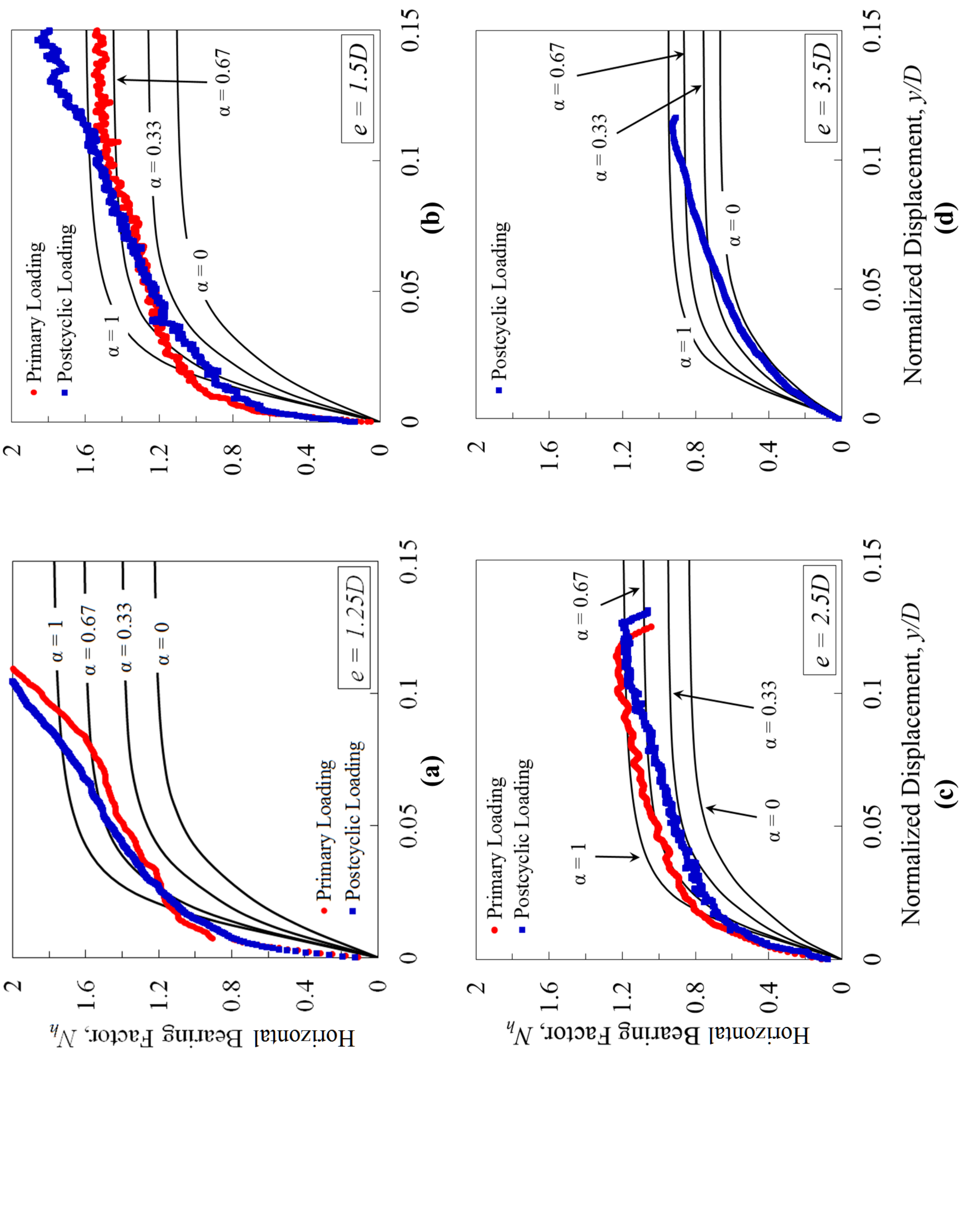

FIG. 8. Comparison of measured data against finite element predictions: (a) e = 1.25D; (b) e = 1.5D; (c) e = 2.5D; (d) e = 3.5D

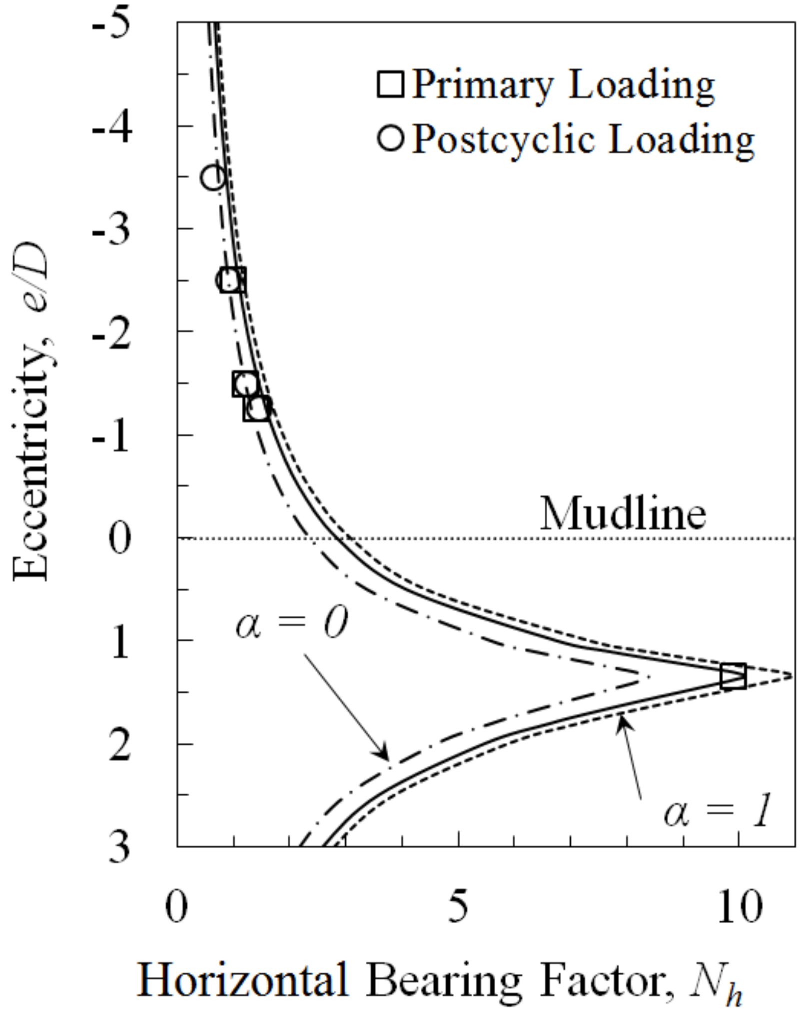

FIG. 9. Effect of eccentricity on horizontal bearing capacity

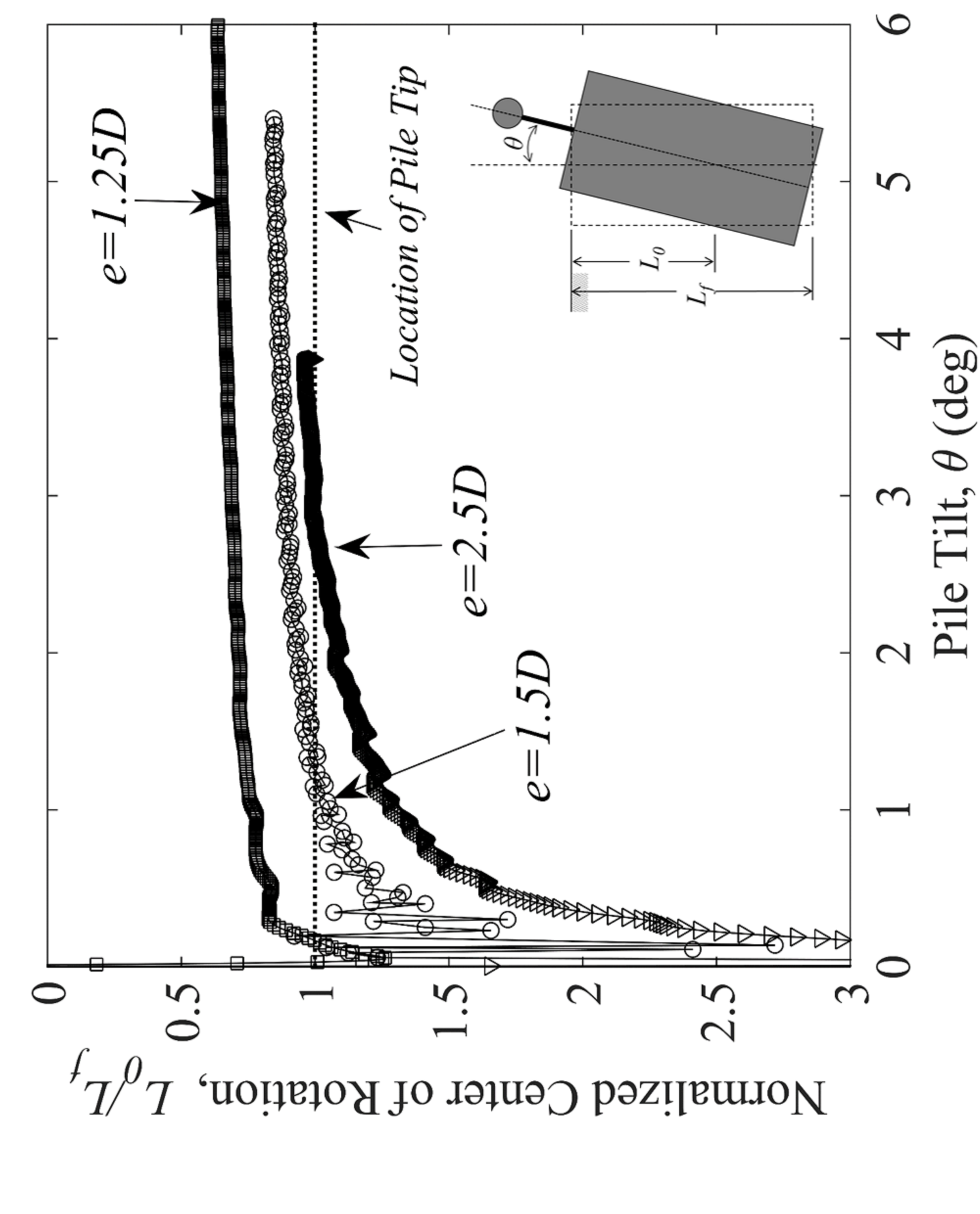

FIG. 10. Variation of center of rotation (primary loading)

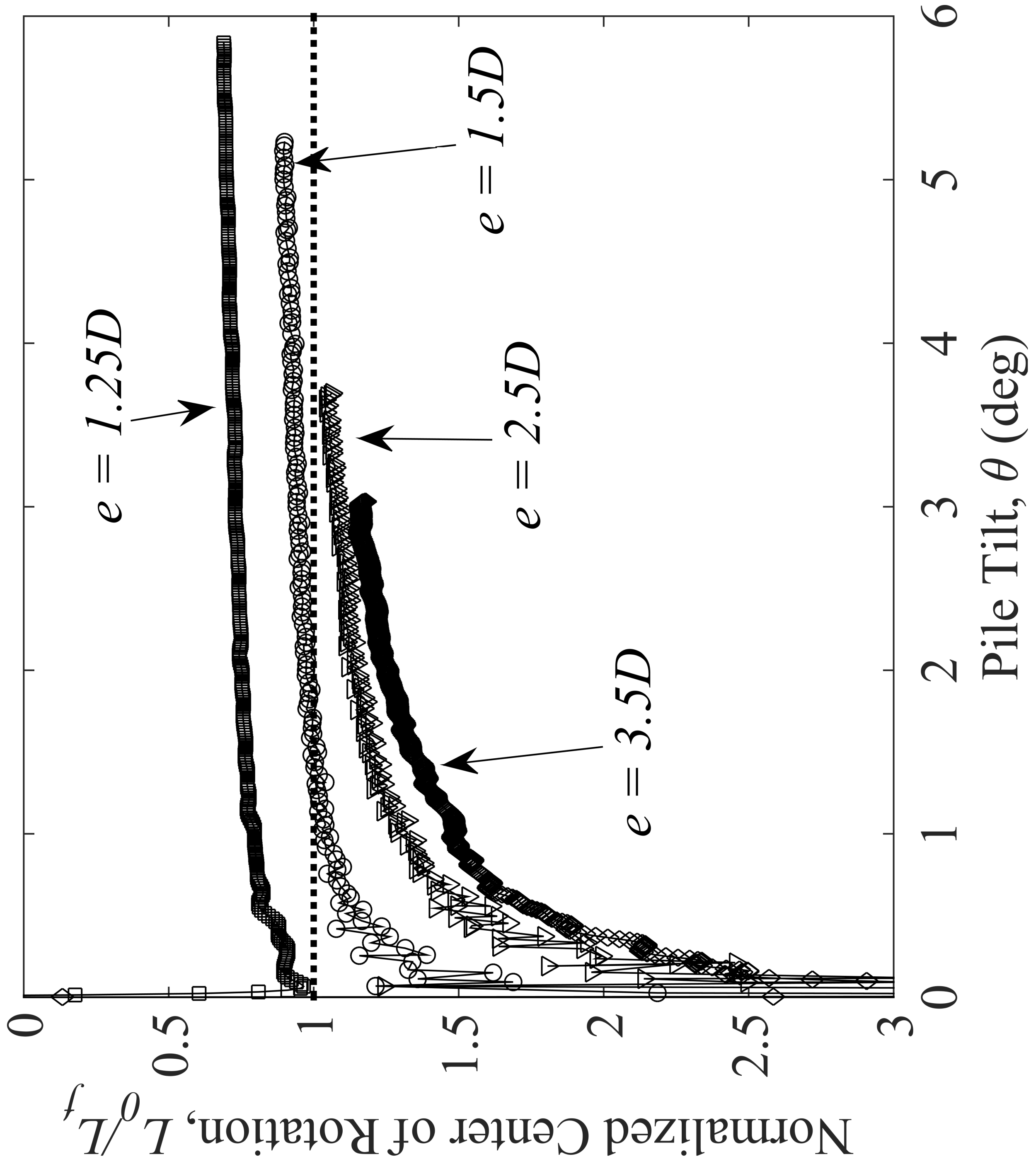

FIG. 11. Variation of center of rotation (post cyclic loading)

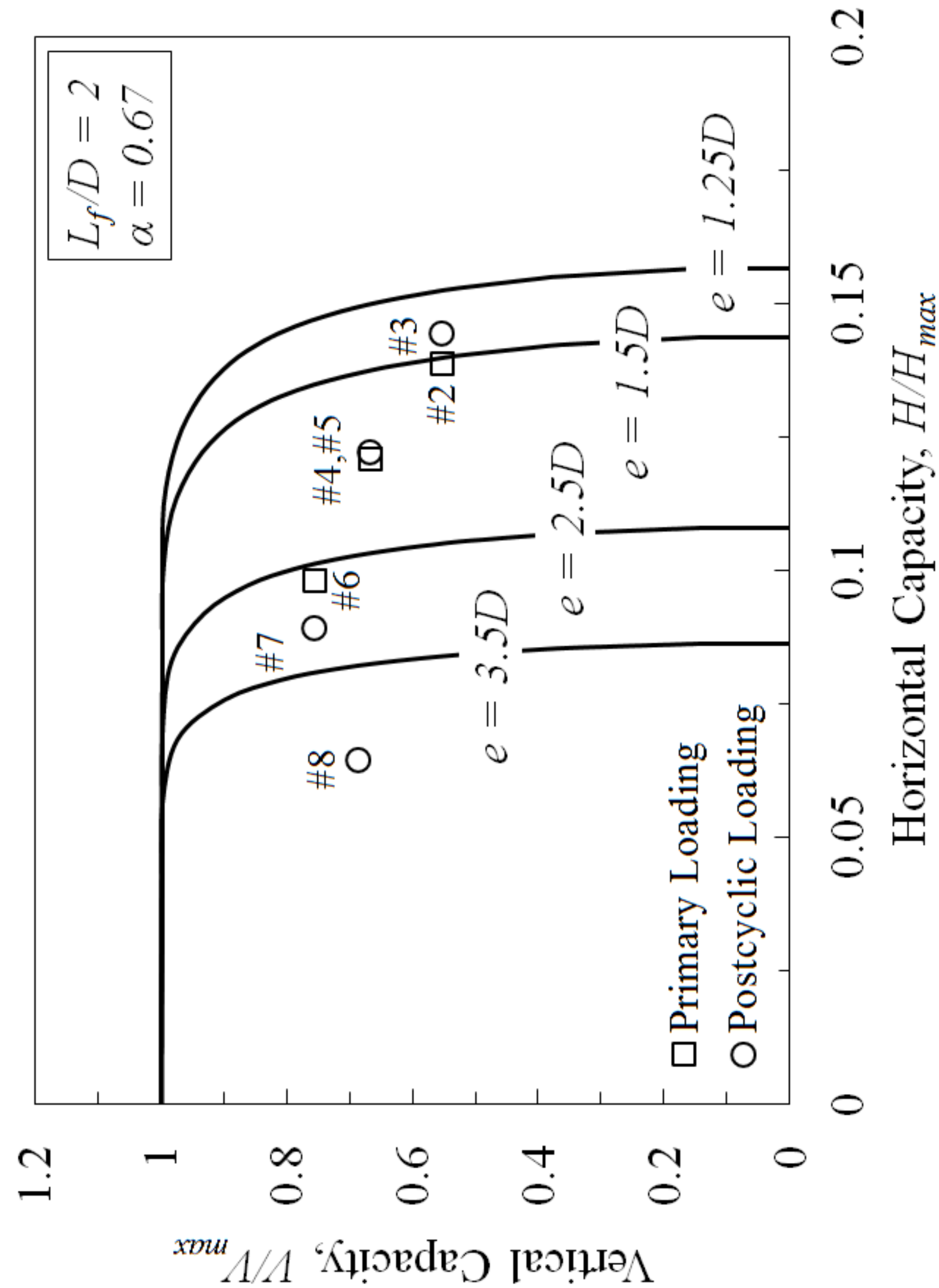

FIG. 12. V-H Comparison of analytical predictions and experimental data.

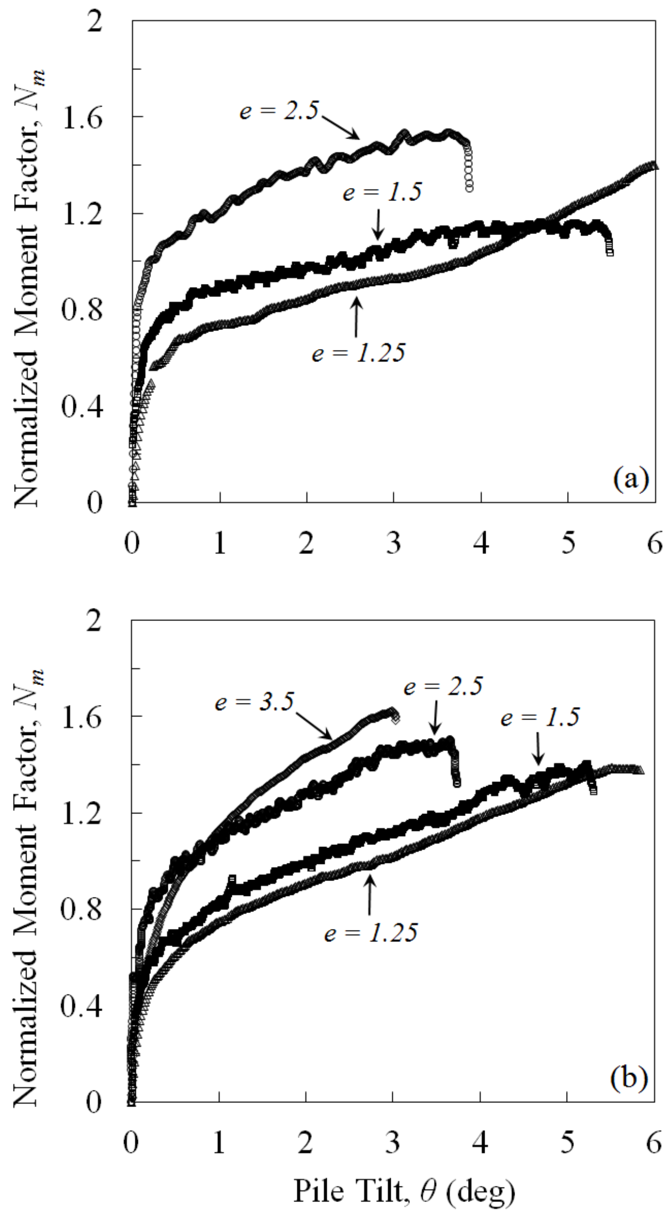

FIG. 13. Moment tilt curves for piles in rotation: (a) primary loading; (b) post cyclic loading;